TR-O-0068 49

GaAsパターン基板上でのGaAsの分子線エピタクシーにおけるGa表面拡散長の異方性

武部　敏彦

1994. 3. 31

ATR光電波通信研究所

ATR Technical Report

報告題名　：　GaAsパターン基板上でのGaAsの分子線エピタクシーにおけるGa表面拡散長の異方性*

報告者　：　武部　敏彦

所属　：　ATR光電波通信研究所　通信デバイス研究室

報告内容概要　：

【1】研究の動機

我々のグループではGaAs(111)A及び(001)パターン基板上に分子線エピタクシー(MBE)でGaAs/AlGaAs多層膜を成長する間に生じるファセットを系統的に研究してきた[#,$]。両方のパターン基板上に共通に発生するファセットを確認すると共に、それぞれのパターン基板上に特有のファセットも観察した。また、各ファセットが側壁傾斜角に依存して発生消滅する様子を明らかにし、成長中にファセットが発生せず、元のパターン形状を維持できる側壁傾斜角の範囲を決定した。

本報告では、上記の研究成果に基づき、パターン基板上での結晶成長過程というより基礎的な側面に注意を向ける。すなわち、具体的には面方位に依存した成長速度及びGa表面拡散長について論じる。これらの異方性は、面方位に依存した表面原子配列と、入射原子と表面原子との相互作用の違いを反映していると考えられる。逆にこの現象が明らかになれば、実験的に観察されたファセット発生の要因、更には(111)A面上で働いている結晶成長機構を物理的に説明できる。また、横方向p-n接合の作製のようなデバイス応用の観点から、(111)Aパターン基板と(001)パターン基板を比較し、その一長一短を検討する。最後に、今回明らかになったGa表面拡散長の異方性から、報告例のほとんどない$(\bar{1}\bar{1}\bar{1})$Bや(110)パターン基板ではどの様に成長するかを議論する。

【2】研究の成果

(111)A及び(001)パターン基板上に共通に発生するファセットとそれぞれのパターン基板上に特有のファセットについて、それらの基板面上での成長速度に対する相対成長速度と、それらに隣接する領域での局在的な成長層厚の変化を詳しく調べることにより、次の様な結果を得た。

1. Ga表面拡散長、λ_{Ga}、は、$\lambda_{Ga}(001) \approx \lambda_{Ga}(\bar{1}\bar{1}3)B < \{\lambda_{Ga}(\bar{1}\bar{1}1)B, \lambda_{Ga}(\bar{3}\bar{3}\bar{1})B, \lambda_{Ga}(013), \lambda_{Ga}(113)A\} < \lambda_{Ga}(159) \approx \lambda_{Ga}(114)A \approx \lambda_{Ga}(111)A \leqq \lambda_{Ga}(110)$なる面方位依存性を示す。すなわち、$\lambda_{Ga}$は、(001)面で最短で、$(\bar{1}\bar{1}\bar{1})$B関連面、(111)A関連面の順で長くなり、(110)面で最長となる。

2. 従って、これらの面が共存した場合、入射したGa原子はλ_{Ga}の長い面からλ_{Ga}の短い面へ拡散して格子に取り込まれるので、(110)ファセットの相対成長速度は極めて低く、ファセットに隣接する(001)面ではGa原子の流入に伴う成長層厚の局在的な増加が必ず見られる。

3. デバイス応用の観点からは、横方向p-n接合の作製では、接合近傍で成長層厚の局在的な増加が必ず見られる短λ_{Ga}の(001)パターン基板より、平坦な成長層が得られる長λ_{Ga}の(111)Aパターン基板の方が単純な構造の横方向p-n接合が得られるので有利である。他方、λ_{Ga}かそれ以下の寸法に対応する量子線や量子点の作製では、短λ_{Ga}の(001)パターン基板の方が、Ga原子の流入による[001]方向の選択的成長と他の方向への成長抑制が利くので有利である。

4. この様に、GaAs基板面方位とGa表面拡散長の異方性を巧妙に組み合せることにより、複雑な構造を簡単なプロセスで作製したり、単純な構造を、余計な構造の発生を抑制して作製することができる。

5. 今回明らかになったGa表面拡散長の異方性から、$(\bar{1}\bar{1}\bar{1})$Bや(110)パターン基板ではどの様なファセットが成長するかについても検討した。

以上

* 本報告は、本文中ではPaper IIIと名付けられている。

ATR Technical Report 「GaAs(111)Aパターン基板上でのGaAs/AlGaAs多層膜の分子線エピタクシー中のファセット成長」(Paper I)。

$ ATR Technical Report 「GaAs(001)パターン基板上でのGaAs/AlGaAs多層膜の分子線エピタクシー中のファセット成長」(Paper II)。

目次

Anisotropic Ga Surface Diffusion in Molecular Beam Epitaxy of GaAs on GaAs Patterned Substrates

-Abstract-

Extra facet generation on ridge-type triangles with (001)-, (110)-, and (201)-related equivalent slopes on GaAs (111)A substrates and stripes running in the [$\bar{1}$10], [110], and [100] directions on (001) substrates during molecular beam epitaxy of GaAs/AlGaAs multilayers was investigated. Growth of extra (114)A, (110), and ($\bar{1}\bar{1}\bar{1}$)B facets was common to the (111)A and (001) patterned substrates. By investigating local variation in layer thickness in the regions adjacent to these facets and extra facets specific to the respective substrates, the orientation-dependent Ga surface diffusion length, λ_{Ga}, was elucidated as $\lambda_{Ga}(001) \approx \lambda_{Ga}(\bar{1}\bar{1}\bar{3})B < \{\lambda_{Ga}(\bar{1}\bar{1}\bar{1})B, \lambda_{Ga}(\bar{3}\bar{3}\bar{1})B, \lambda_{Ga}(013), \lambda_{Ga}(113)A\} < \lambda_{Ga}(159) \approx \lambda_{Ga}(114)A \approx \lambda_{Ga}(111)A \leqq \lambda_{Ga}(110)$.

Considering application of patterned substrates to the fabrication of lateral p-n junctions, the present result that $\lambda_{Ga}(001)$ is the shortest may limit the use of (001) substrates because an exponential variation of the layer thickness always appears on the (001) substrate plane at the boundary with the sidewall and hampers the formation of simple structures. In contrast, (111)A and (110) substrates with relatively long λ_{Ga} are free from such a limitation, and hence may be more suitable for such applications, although epitaxial growth of good layers on (111)A and (110) surfaces is very difficult. On the other hand, the (001) substrate will be suitable for the formation of quantum wires and dots on patterns with dimensions around λ_{Ga} because the preferential incorporation of Ga

adatoms into the (001) surface leads to enhancement of the growth rate in the (001) direction and suppression of the growth rates in the other directions.

Key words : gallium arsenide, aluminum gallium arsenide, patterned substrate, molecular beam epitaxy, crystal facet, diffusion length.

1. Introduction

In the preceding two papers designated as Paper I and Paper II, facet generation behaviors during molecular beam epitaxy (MBE) of GaAs/AlGaAs multilayers on (111)A and (001) patterned substrates with sidewalls of various orientations and slopes have been investigated. The extra facets that commonly generate on both substarates have been identified, together with those observed on respective substrates. The generation behavior of each facet with respect to the slope of the sidewall has been elucidated and the ranges of the slope for which no extra facets generate during MBE and layers can be grown with maintaining the initial as-eched patterns have been determined.

In the present paper, designated as Paper III, we focus on more fundamental aspects of growth on patterned substrates, that is, we discuss the orientation-dependent growth rate and Ga surface diffusion length, based on the results and discussion in the preceding papers. These anisotropies reflect the orientation-dependent surface atomic configuration and the difference in the interaction of incident atoms with the surface atoms. This, in turn, can physically explain the observed facet generation behaviors and also the growth mechanisms working on the (111)A surface. We also discuss the merits and demerits of the (111)A and (001) patterned substrates in view of device application such as fabrication of lateral p-n junctions [1-11]. Finally, we make some comments on growth behaviors expected on $(\bar{1}\bar{1}\bar{1})$B and (110) patterned substrates

2. Data analysis and Evaluation

The fabrication of the GaAs (111)A and (001) patterned substrates, MBE growth of the GaAs/AlGaAs multilayers on these substrates, and observation of the grown layers by scanning electron microscopy (SEM) have been described in Paper I and Paper II.

Growth of extra (114)A, (110), and $(\bar{1}\bar{1}\bar{1})$B facets was confirmed as common to the (111)A and (001) patterned substrates in Paper II, as summarized in Figure 1. Note the identical surface morphologies of these facets on the (111)A and (001)

patterned substrates. Extra (113)A, (001), and (159) facets on the (111)A patterned substrates and extra (111)A, $(\bar{1}\bar{1}\bar{3})$B, and (013) facets on the (001) patterned substrates also were confirmed as main facets. The intersection angle with the substrate plane, θ_f, and the growth rate relative to that on the substrate plane, R'[lmn], for each facet were evaluated from the SEM images according to the procedure described in the Appendix.

The GaAs/AlGaAs multilayers simultaneously grown on (111)A and (001) planar substrates exhibited the same growth rates, R, that is,

R[111]A = R[001].

Under the present high As_4 pressure growth condition, R is controlled by the Ga and Al flux intensities.

The above equality was also confirmed to be true for the simultaneously grown GaAs/AlGaAs multilayers on the substrate planes far from the patterns on the (111)A and (001) patterned substrates. It has been reported that the simultaneously grown GaAs/AlGaAs multilayers on (110) and (001) planar substrates exhibited the same growth rates [12], that is,

R[110] = R[001].

The orientation-dependent growth rate, therefore, has meaning for systems where there exist interactions of adatoms among two or more different coexisting surfaces, especially for the adjacent substrate plane - facet - sidewall system. In evaluating the relative growth rate, that the effective molecular beam fluxes differ for the substrate plane, the facet, and the sidewall, and that the Ga surface diffusion length, λ_{Ga}, critically depends on the As_4 flux and growth temperature, must be taken into consideration. In [13-17], λ_{Ga} on the (001) surface, $\lambda_{Ga}(001)$, has been reported to shorten as the growth temperature decreases and/or the As_4 pressure increases. One simple expression of the variation of the effective molecular beam fluxes with θ is the "cosine law" and if no interactions of adatoms between two adjacent surfaces are assumed, the relative growth rate, R"[lmn], of the facet is expressed as

R"[lmn] = $\cos\theta_f$.

A deviation of R'/R" from unity represents a simple measure of the strength of the interactions between the adjacent surfaces and the orientation-dependent incorporation of adatoms.

Table 1 summarizes the values of R', R", and R'/R" for the facets reported in Paper I and Paper II. Accurate values of R's could be obtained by averaging over several points on a sample. The value of R' for each facet did not vary with θ but varied when there was another facet adjacent to the facet in question, like the (159) facet listed in the table (see Paper I).

3. Results and Discussion

1. Anisotropy of Ga surface diffusion length and facet growth rate

In the system of substrate plane - facet - sidewall, exponential thickness variations of the layers grown on the substrate plane and/or on the sidewall towards the boundary with the facet reflect the anisotropy of λ_{Ga} depending on the surface orientation. Since Ga adatoms incident on a substrate where variously oriented surfaces are exposed migrate towards a surface with the minimum λ_{Ga} and are incorporated there, it follows that a surface showing an exponential thickness variation of the layer towards the adjacent surfaces has a shorter λ_{Ga} than the adjacent surfaces. For a facet with a longer λ_{Ga}, the saturated lateral length of the facet, estimated after fully long growth, may give a rough estimate of λ_{Ga} on the facet. For a substrate plane or sidewall with a longer λ_{Ga}, the value of λ_{Ga} cannot be evaluated. By studying these points for the substrate plane - facet - sidewall systems reported in Paper I and Paper II, orientation dependence of λ_{Ga} is deduced.

(1) (111)A, (11N)A, and (001) surfaces

Figure 2 shows cross-sectional profiles of the (111)A sidewall of the [$\bar{1}$10] stripe and the (001) sidewall of the (001) triangle. Generation of the (114)A facet was confirmed on both patterned substrates. In (a), an exponential thickness variation was observed for the layers grown on the (001) substrate plane towards the boundary with the (114) facet, while there was no such variation on the (111)A

sidewall. The same result has been repoted in many papers studying the growth on [$\bar{1}$10] stripes on (001) substrates [3-5, 15, 18-23]. In (b), an exponential thickness variation of the layers grown on the (001) sidewall was observed towards the boundary with the (114) facet, while there was no such variation on the (111)A substrate plane. These results consistently imply that some of the Ga atoms incident on the (111)A surface migrated to the (001) surface through the (114)A surface and finally were incorporated in the lattice within a characteristic distance λ_{Ga} from the boundary. The interchange of the roles of substrate plane and sidewall between the (111)A and (001) surfaces, however, might lead to different results since the effective beam fluxes and flux ratio are different between the substrate plane and sidewall, and λ_{Ga} is affected by such a growth ambience [13-17]. The significance of the present results is that we have clearly confirmed for the first time that the experimental evidence obtained on (001) patterned substrates that λ_{Ga}(111)A is longer than λ_{Ga}(001) essentially originates from the crystalline anisotropy and applies to all (111)A-(001) systems.

Since the (11N)A surface (N=1, 2, 3,--) is composed of the (111)A and (001) elements, λ_{Ga}(11N)A will have a value intermediate between λ_{Ga}(111)A and λ_{Ga}(001). Figure 3(a) shows the generation of the ($\bar{1}\bar{1}$3)A facet with θ_f=80° adjacent to the (114)A facet on the ($\bar{2}\bar{2}$5)A sidewall of the (001) triangle. The R'/R" for the ($\bar{1}\bar{1}$3)A facet was much larger than unity as listed in Table 1. These show the Ga migration from the (111)A substrate plane to the ($\bar{1}\bar{1}$3)A facet. The generation of the (113)A facet with θ_f=30° adjacent to the (110) facet on the (110) triangle (shown below) with R enhanced even over R[111]A (Table 1) indicates the preferential incorporation into the (113)A facet of Ga adatoms migrating from the (110) facet to the (111)A substrate plane. These results are strong evidence that λ_{Ga}(113)A is shorter than λ_{Ga}(111)A. The R'/R" for the (114)A facet is slightly lower than unity on both the (111)A and (001) patterned substrates (Table 1), which is responsible for the appearance of the facet itself and the exponential thickness variation of the layers on the (001) and (11N)A surfaces adjacent to the facet. This suggests that λ_{Ga}(114)A is comparable to

λ_{Ga}(111)A surface. Thus, the dependence of λ_{Ga}(11N)A on N is not simple. Taking into consideration the whole data on the growth on the (11N)A sidewalls in the (111)A and (001) patterned substrates shown in Paper I and Paper II, it was roughly concluded that, with respect to the Ga surface diffusion, the (11N)A surfaces with $N \leqq 6$ behave like "the (111)A surface" and the (11N)A surfaces with $N \geqq 7$ behave like "the (001) surface". Consistent with this conclusion, no thickness variation of the layers grown on the (001) substrate plane was observed adjacent to the (11N)A facets with $N=9$ and 13 on the intersection of the [100] and [010] stripes (see Figures 17(g) and (h) in Paper II), as exemplified for the (119)A facet in Figure 4.

Figure 3(b) shows a cross-sectional profile of the $(\bar{2}\bar{2}5)$A sidewall of the (001) triangle. Generation of the (001) facet was confirmed. The R'/R" for the (001) facet is sligtly higher than unity, which is responsible for the appearance of the facet itself (the condition for facet generation at a concave intersection of the sidewall with the lower substrate plane is opposite to that at a convex intersection of the sidewall with the upper substrate plane). This indicates that excess Ga atoms migrated from the lower (111)A substrate plane and/or $(\bar{2}\bar{2}5)$A sidewall (more generally the $(\bar{N}\bar{N}M)$A sidewalls) and were preferentially incorporated on the (001) surface, which gives another evidence consistent with the above discussion that λ_{Ga}(001) is shorter than λ_{Ga}(111)A and λ_{Ga}(11N)A (the $(\bar{1}\bar{1}N)$A surface is equivalent to the (11N)A surface and the $(\bar{2}\bar{2}5)$A surface is included in the (11N)A series).

Figure 5 shows cross-sectional profiles of the (445)A and (335)A sidewalls of the $[\bar{1}10]$ stripes. Generation of the (111)A facet was confirmed on both sidewalls. Figure 5(a) corresponds to Figure 4(b) in Paper II, that is, the sidewall with the characteristic step structures and Figure 5(b) to Figure 4(c) in Paper II, that is, the sidewall without them. In (a), only steps composed of the (011)-related and (101)-related facets are observed at the (111)A facet - (445)A sidewall layer boundary. On the other hand, in (b), an exponential thickness variation of the layers on the (335)A sidewall towards the (111)A facet is clearly observed. This

structural transition of the (111)A facet - sidewall layer boundary is interesting since it should reflect Ga adatom migration in the competition of λ_{Ga} on the sidewall with the width of the microsteps on the as-etched sidewall, but is not discussed here. The R'/R" for the (111)A facet is much lower than unity (Table 1), which is responsible for the appearance of the facet itself and evidences that excess Ga atoms migrated from the (111)A facet to the adjacent (335)A sidewall and (001) substrate plane and were incorporated there. This also consistently confirms that λ_{Ga}(111)A is longer than λ_{Ga}(001) and λ_{Ga}(11N)A.

(2) (110) and $(\bar{N}\bar{N}\bar{1})$B surfaces

Figure 6 shows cross-sectional profiles of the (010) sidewall of the [100] stripe, the $(33\bar{1})$B sidewall of the (110) triangle, and the $(\bar{2}14)$ sidewall with an inverted mesa of the (210) triangle. Generation of the (110) facet was confirmed on all of the patterns (the (011) and $(\bar{1}01)$ surfaces are equivalent to the (110) surface). The R'/R" for the (110) facet evaluated from Figures 6(a) and (b), listed in Table 1, is extremely low on both of the (001) and (111)A patterned substrates, which suggests a long λ_{Ga} on the (110) surface and that the Ga atoms incident on the (110) facet migrated to the adjacent sidewall and substrate plane and were incorporated there. In (a), an exponential thickness variation of the layers grown on the (001) substrate plane was observed towards the boundary with the (011) facet. This means that λ_{Ga}(110) is longer than λ_{Ga}(001). In (b), an exponential thickness variation of the layers grown on the $(33\bar{1})$B sidewall towards the boundary with the (110) facet was observed and the (113)A facet was formed on the (111)A substrate plane adjacent to the (110) facet. Since the generation of the (113)A facet instead of an exponential thickness variation is due to preferential incorporation of Ga atoms into the (113)A surface, as discussed in (1), the result leads to the conclusion that λ_{Ga}(110) is longer than $\lambda_{Ga}(\bar{3}\bar{3}\bar{1})$B, λ_{Ga}(113)A, and λ_{Ga}(111)A. The first inequality can be extended so as to include $\lambda_{Ga}(\bar{N}\bar{N}\bar{1})$B (N=1, 2, 3,--) on the basis of the experimental results shown in Figure 9 in Paper I, which is quite natural considering that the $(\bar{N}\bar{N}\bar{1})$B surface is composed

of the $(\bar{1}\bar{1}0)$ and $(\bar{1}\bar{1}\bar{1})$B elements and the general trend of λ_{Ga}(11N)A discussed in (1).

It should be noted in Figure 6(c) that no exponential thickness variation was observed for the layers grown on the (111)A substrate plane towards the boundary with the $(\bar{1}01)$ facet. The R' of the $(\bar{1}01)$ facet evaluated from Figure 6(c), also listed in Table 1, was very much enhanced, which leads to the conclusion that λ_{Ga}(111)A is comparable with or longer than λ_{Ga}(110). This conclusion is inconsistent with the conclusion obtained above. In Paper I, we pointed out that the $(\bar{1}01)$ facet generation depended on the presence of the inverted mesa because the facet did not appear on the sidewalls that consisted only of normal mesas with similar θ values. This result suggests that the Ga surface diffusion process was affected by the profile between the substrate plane and the sidewall. The large difference in the value of θ_f, 35 ° for the (110) facet but 90 ° for the $(\bar{1}01)$ facet, may also be responsible for the discrepancy because the effective molecular beam fluxes and flux ratio greatly change with θ_f and λ_{Ga} critically depends on these growth ambiences [13-17]. Therefore, we conclude tentatively that λ_{Ga}(110) is comparable with or longer than λ_{Ga}(111)A.

Figure 7(a) shows a top view of the corner of the (001) triangle with the (001) sidewalls (θ=54 °) after growth. The (110) facet on the corner is observed together with the (001) sidewall layer and the (114)A facet. A close check of this figure confirmed that the (114)A facet and the (001) sidewall layer changed their thicknesses exponentially towards the (110) facet. In fact, Note that the relation of the (110) facet to the (001) sidewall in this figure is exactly the same as the relation of the (011) facet to the (001) substrate plane shown in Figure 6(a). This leads to the conclusion that λ_{Ga}(110) is longer than λ_{Ga}(001) and λ_{Ga}(114)A, consistent with the previous discussion. Figure 7(b) shows a top view of the corner of the (021) triangle with the $(\bar{2}38)$ sidewalls (θ=55 °) after growth. The (110) facet on the corner is observed together with the (159) facet. It was confirmed by a similar check that the (159) facet changed its thickness

exponentially towards the (110) facet. This leads to the conclusion that $\lambda_{Ga}(110)$ is longer than $\lambda_{Ga}(159)$.

(3) $(\bar{1}\bar{1}\bar{1})$B and $(\bar{1}\bar{1}\bar{N})$B surfaces

Figures 8 shows cross-sectional profiles of the $(\bar{1}11)$B sidewall with an inverted mesa of the [110] stripe and the $(77\bar{8})$B sidewall of the (110) triangle. Generation of the $(\bar{1}\bar{1}\bar{1})$B facet was confirmed on both patterns. In (a), an exponential thickness variation of the layers grown on the (001) substrate plane was observed towards the boundary with the $(\bar{1}11)$B facet, which means that $\lambda_{Ga}(\bar{1}\bar{1}\bar{1})$B is longer than $\lambda_{Ga}(001)$. The R'/R" for the $(\bar{1}11)$B facet on the (001) patterned substrate is much lower than unity, as listed in Table1. This strongly suggests a lateral migration to the (001) substrate plane of excess Ga adatoms not incorporated on the initially formed $(\bar{1}11)$B plane. Similar results have been presented in previous reports [18, 24, 25]. The R'/R" for the $(11\bar{1})$B facet on the (111)A patterned substrate was larger than unity, as listed in Table 1. Since the growth rate on $(\bar{1}\bar{1}\bar{1})$B substrates is suppressed as the As_4 pressure increases [26], this is strong evidence of the lateral Ga migration from the (111)A substrate surface to the sidewall. This excess Ga supply from the (111)A substrate surface reduced the effective V/III flux ratio, and hence favored the growth of the $(11\bar{1})$B facet. Thus, it can be safely concluded that $\lambda_{Ga}(111)$A is longer than $\lambda_{Ga}(\bar{1}\bar{1}\bar{1})$B although no exponential thickness variations on the facet were observed in (b).

Figure 9 shows a cross-sectional profile of the $(\bar{1}12)$B sidewall of the [110] stripe. Generation of the $(\bar{1}13)$B facet was confirmed. The generation of the $(\bar{1}\bar{1}\bar{3})$B facet has been reported in [27] in the lateral growth of GaAs on $(\bar{1}\bar{1}\bar{1})$B patterned substrates under high As_4 pressures by metalorganic MBE (MOMBE). The R'/R" for the $(\bar{1}13)$B facet is slightly lower than unity (Table 1), which is responsible for the appearance of the facet itself. It should be noted that no exponential thickness variations of the layers grown on the (001) substrate plane were observed towards the boundary with the $(\bar{1}13)$B facet in contrast to the $(\bar{1}11)$B facet. This means that $\lambda_{Ga}(\bar{1}\bar{1}\bar{3})$B is comparable to $\lambda_{Ga}(001)$. Therefore, considering that the $(\bar{1}\bar{1}\bar{N})$B surface is composed of the $(\bar{1}\bar{1}\bar{1})$B and $(00\bar{1})$ ele-

ments, $\lambda_{Ga}(\bar{1}\bar{1}\bar{N})B$ will decrease as N increases in accordance with $\lambda_{Ga}(11N)A$. Since $\lambda_{Ga}(113)A$ was longer than $\lambda_{Ga}(001)$ as discussed in (1), $\lambda_{Ga}(11N)A$ will generally be longer than $\lambda_{Ga}(\bar{1}\bar{1}\bar{N})B$. In fact, this idea is consistent with the conclusion made above that $\lambda_{Ga}(111)A$ is longer than $\lambda_{Ga}(\bar{1}\bar{1}\bar{1})B$.

(4) (013) surface

Figure 10 shows a cross-sectional profile of the (045) sidewall of the [100] stripe. Generation of the (013) facet was confirmed. An exponential thickness variation of the layers grown on the (001) substrate plane is observed towards the boundary with the (013) facet. This means that $\lambda_{Ga}(013)$ is longer than $\lambda_{Ga}(001)$. The R'/R" for the (013) facet is slightly lower than unity, which is responsible for the appearance of the facet itself and the exponential thickness variation of the layers on the (001) substrate plane adjacent to the facet.

It has been shown in [28] that the (011) and (013) facet coexist in growth under low temperatures and/or high As_4 pressures. This implies that $\lambda_{Ga}(110)$ decreases faster than $\lambda_{Ga}(013)$ as the growth temperature decreases and/or the As_4 pressure increases.

(5) (159) surface

Figure 11 shows a cross-sectional profile of the $(\bar{3}27)$ sidewall of the (201) triangle. Generation of the (159) facet was confirmed. The R'/R" for the (159) facet is close to unity when the $(\bar{1}01)$ and $(\bar{1}25)$ facets are adjacent to the (159) facet while it is much lower than unity when the $(\bar{2}38)$ facet is adjacent to the (159) facet, as listed in Table 1 (see also Figure 16 in Paper I). The R'/R"s for the $(\bar{1}01)$ and $(\bar{1}25)$ facets are greatly enhanced over unity and the R'/R" for the $(\bar{2}38)$ facet is slightly lower than unity. No exponential thickness variations of the layers grown on the (111)A substrate plane were observed towards the boundary with the (159) facet in either case. Thus, the present results clearly indicate that an excess of the Ga atoms incident on the (111)A substrate plane finally migrated through the (159) facet to the adjacent sidewall and were incorporated there independent of the facets adjacent to the (159) facet, and hence, $\lambda_{Ga}(159)$ is comparable to or shorter than $\lambda_{Ga}(111)A$. The R' for the (159)

facet which varies depending on the adjacent facet is very interesting in that the Ga migration on the sidewall is controlled in competition between multiple adjacent facets. To date, this phenomenon has not been reported so far because usually only a single facet generates.

Table 2 summarizes the orientation dependence of λ_{Ga} discussed above. The inequalities expressing the order of λ_{Ga} are consistently unified to a single inequality as follows:

$\lambda_{Ga}(001) \approx \lambda_{Ga}(\bar{1}\bar{1}\bar{3})B < \{\lambda_{Ga}(\bar{1}\bar{1}\bar{1})B, \lambda_{Ga}(\bar{3}\bar{3}\bar{1})B, \lambda_{Ga}(013), \lambda_{Ga}(113)A\} < \lambda_{Ga}(159) \approx \lambda_{Ga}(114)A \approx \lambda_{Ga}(111)A \leqq \lambda_{Ga}(110)$.

That is, λ_{Ga} increases in the order of the (001), $(\bar{1}\bar{1}\bar{1})$B-related, (111)A-related, and (110) surfaces. Since the (013) facet is composed of the (011) and (001) elements and the (159) facet is composed of the $(\bar{1}01)$ and (111)A elements, the locations of $\lambda_{Ga}(013)$ and $\lambda_{Ga}(159)$ in the above inequality are reasonable. We did not include $\lambda_{Ga}(\bar{2}38)$ or $\lambda_{Ga}(\bar{1}25)$ in the above inequality because the $(\bar{2}38)$ and $(\bar{1}25)$ facets are dependent on the existence of the (159) facet.

The above order is interesting for the following reasons:

① Since the (001) and (110) surfaces are nonpolar while the (111)A and $(\bar{1}\bar{1}\bar{1})$B surfaces are polar, the above order does not reflect the strength of surface polarity.

② Considering that the $(\bar{1}\bar{1}\bar{1})$B growth favors low As_4 pressures [29-35] while the (110) and (111)A growth favors high As_4 pressures [36-43], the above order may reflect the strength of As_4 sticking on the surface. It is well known that the As_4 sticking coefficient is very low on the (111)A and (110) surfaces [36, 37, 44].

③ The (110) and (111)A-related surfaces with a relatively long λ_{Ga} show amphoteric Si doping nature [36, 37, 41, 45-58] while the (001) and $(\bar{1}\bar{1}\bar{1})$B-related surfaces with a relatively short λ_{Ga} show only n-type Si doping nature [29, 34, 35, 44, 50-56, 59]. This strongly suggests that Si doping characteristics depend on the Ga surface diffusion, which is in good accordance with the fact that the amphotericity of Si doping shifts towards n-type doping and the value of λ_{Ga} shortens as the As_4 pressure increases [13-15, 17].

④ The order also corresponds well to the general trend of difficulty of growing epitaxial layers with good crystalline quality. The (001) surface is most widely used for epitaxial growth of various materials both in basic research and in mass-production because of the ease of obtaining good epitaxial layers over wide growth conditions. On the other hand, as we move to the $(\bar{1}\bar{1}\bar{1})$B, (111)A, and (110) surfaces, the condition for good epitaxial growth becomes more limited than or further shifted from the (001) growth condition. As_4 pressures higher than those for the (001) growth are required for the (111)A and (110) growth for example [36-43], which may correspond to reducing the effective λ_{Ga} on these surfaces and making them closer to $\lambda_{Ga}(001)$. The $(\bar{1}\bar{1}\bar{1})$B growth favors low As_4 pressures or low growth rate processes such as migration-enhanced epitaxy (MEE) [29-35, 60], which seemingly makes $\lambda_{Ga}(\bar{1}\bar{1}\bar{1})$B longer. These growth conditions, however, are taken because otherwise excess As_4 molecules form As trimers in the (2×2) reconstruction on the $(\bar{1}\bar{1}\bar{1})$B surface and hamper further $(\bar{1}\bar{1}\bar{1})$B growth [31-33]. Thus, these factors specific to the $(\bar{1}\bar{1}\bar{1})$B surface must be taken into consideration together with $\lambda_{Ga}(\bar{1}\bar{1}\bar{1})$B in considering the $(\bar{1}\bar{1}\bar{1})$B growth.

⑤ As to the solution growth of bulk GaAs crystals, crystals are pulled in the [001] direction using (001) seeds in the liquid-encapsulated Czhocralski method while they are grown in the $[\bar{1}\bar{1}\bar{1}]$B direction using $(\bar{1}\bar{1}\bar{1})$B seeds in the horizontal Bridgman method. These may correspond to using short-λ_{Ga} surfaces, although the growth conditions and mechanisms are quite different between solution growth and MBE. From this and the discussion in ④, the obtained orientation dependence of λ_{Ga} seems to reflect orientation dependence of the surface energy for Ga adatoms, that is, the surface energy increases in the order of the (001), $(\bar{1}\bar{1}\bar{1})$B-related, (111)A-related, and (110) surfaces.

⑥ In Paper I, generation of the (110) and (NNM)A facets (N=2, 3, --; M≧N/2) on the corners of the (001) and (201) triangles on the (111)A substrates was reported. The preferential generation of these facets is due to their long λ_{Ga}s and very low growth rates (note that the (NNM)A surface is composed of the (110) and (111)A elements). As the inequality on N and M shows, (NNM)A does

include (221)A but does not include, for example, (331)A. Since the (331)A plane is located between the (110) and (221)A planes, the above λ_{Ga} order should force the (331)A facet to also appear on the corners of the (001) and (201) triangles. Consider the case of the (001) triangle. The θ corresponding to the θ_f of the (221)A facet, 16 °, is 29 ° and corresponds to the 1 °-misoriented (113)A sidewall. The θ corresponding to the θ_f of the (331)A facet, 22 °, is 39 ° and coreresponds to the (115)A sidewall. Since it is reasonable to assume that λ_{Ga}(221)A is longer than λ_{Ga}(113)A and λ_{Ga}(331)A longer than λ_{Ga}(115)A from the above order, the generation of the (221)A and (331)A facets should occur naturally. The (331)A facet, however, was not observed. The reason is unclear at present.

Quantitative evaluation of the values of λ_{Ga}s included in the above inequality will be made in a separate paper.

2. Comparative evaluation of (111)A and (001) patterned substrates

In the previous section, the orientation dependence of λ_{Ga} was elucidated from comparison of the facet generation between the (111)A and (001) patterned substrates. In this section, we compare the facet generation in view of device application of the patterned substrates.

(1) Systems consisting of (111)A and (001) surfaces

We first focus on the systems consisting of (111)A and (001) surfaces, discussed in 2-(1), which have been used for the formation of lateral p-n junctions by growing Si-doped GaAs [1-11] and lateral p-n subband junctions by growing Si-atomic planar-doped GaAs layers or GaAs/AlGaAs quantum wells with selective Si-atomic planar doping to the GaAs wells [61].

In order to obtain flat and uniform layers across the sidewall - substrate plane, θ must be smaller than 10 ° for the [$\bar{1}$10] stripe on the (001) substrate while θ must be in the range of 33 ° to 16 ° for the [$\bar{1}$10] stripe on the (111)A substrate. The sidewall meeting the above condition is (118)A (θ=10 °) for the [$\bar{1}$10] stripe on the (001) substrate and (113)A (θ=30 °) for the [$\bar{1}$10] stripe on the (111)A substrate for example. Since the (118)A plane is very close to the (001) plane, amphoteric Si doping characteristics may not be expected on the (118)A plane.

On the other hand, it has already been established that amphoteric Si doping characteristics give rise to p-type conduction for the (111)A surface and simultaneously to n-type conduction for the (113)A surface under the present growth conditions [9-11]. For the same unit step height, the lateral spread of the sidewall is $\cot 10° = 5.7$ for the $[\bar{1}10]$ stripe on the (001) substrate and $\cot 30° = 1.7$ for the $[\bar{1}10]$ stripe on the (111)A substrate. Thus, the above limitation to θ may be a much larger obstacle to obtaining steep lateral p-n junctions by Si-doping and high-density lateral integration for the $[\bar{1}10]$ stripe on the (001) substrate than for the $[\bar{1}10]$ stripe on the (111)A substrate.

It is also interesting to compare the orientations and cross-sectional profiles of the substrate layer - (114)A facet and (114)A facet - sidewall layer interfaces between the (001) and (111)A patterned substarates. As demonstrated in Figure 2, the flat (111)A layer - (114)A facet interface and the curved (114)A facet - (001) layer interface are common to the two patterned substrates. The two interfaces incline more to the (111)A substrate plane side for the (111)A patterned substrate, while they incline more to the (001) substrate plane side for the (001) patterned substrate. In particular, The (111)A layer - (114)A facet interface is oriented in the $[\bar{1}\bar{1}2]$A direction, that is, perpendicular to the (111)A substrate plane, for the (111)A patterned substrate, while it is oriented in the [110] direction, that is, perpendicular to the (001) substrate plane, for the (001) patterned substrate. If we compare Figure 3 in Paper I and Figure 3 in Paper II, we can summarize the interface behavior with respect to θ as follows:

① For the (111)A patterned substrates, the orientation of the (111)A layer - (114)A facet interface and the (111)A layer - (11N)A sidewall layer interface in the absence of the (114)A facet is almost fixed to the $[\bar{1}\bar{1}2]$A direction independent of θ, while the orientation of the (114)A facet - (11N)A sidewall layer interface changes with the lateral development of the (114)A facet with decreasing θ.

② For the (001) patterned substrates, the (001) layer - (114)A facet interface has a fixed orientation and a profile independent of θ, and the (001) layer - (11N)A

sidewall layer interface in the absence of the (114)A facet becomes flat and oriented in the [110] direction, while the (114)A facet - (11N)A sidewall layer interface inclines more to the (11N)A sidewall with the lateral development of the (114)A facet with decreasing θ.

This asymmetrical interface behavior between the (111)A and (001) patterned substrates can be attributed to the R's of the (114)A facet and (11N)A sidewall layer which roughly follow the cosine θ law and to the directional migration of Ga adatoms from the (111)A (-related) surface to the (001) (-related) surface:

① For the (111)A patterned substrates, since $R[114]A \approx R[111]A\cos\theta_f$ and $R[11N]A \approx R[111]A\cos\theta$, and the (114)A facet develops farther from the (111)A layer - (114)A facet interface, the (111)A layer is smoothly connected to the (114)A facet and the (11N)A sidewall layer without changing the orientation of the interface with the (111)A layer.

② For the (001) patterned substrates, since, although $R[114]A \approx R[001]\cos\theta_f$ and $R[11N]A \approx R[001]\cos\theta$ hold, the (114)A facet develops towards the (114)A facet - (11N)A sidewall layer interface, the interface orientation must change depending on θ for a smooth connection of the (114)A facet with the (11N)A sidewall layer.

Therefore, the flat and θ-independent $[\bar{1}\bar{1}2]$A-oriented interface between the (111)A layer and the (114)A facet (or (11N)A sidewall layer) on the (111)A patterned substrate is more favorably utilized for obtaining simple device structures compared with the corresponding interface on the (001) patterned substrates.

The fact that the (001) layer - (114)A facet interface for the (001) patterned substrate and the (114)A facet - (11N)A sidewall layer interface for the (111)A patterned substrate are curved, may be related to the exponential thickness variations of the adjacent layers. It is because the (110) facet - (NN$\bar{1}$)B sidewall layer interface for the (111)A patterned substrate (Figure 6(b), and Figures 9(b)-(f) in Paper I) is also curved and there is an exponential thickness variation for the sidewall layer adjacent to the interface.

The (11N)A sidewall layer showed poor surface morphologies except for the (114)A facet on the (001) patterned substrate (Figures 4 and 15 of Paper II), whereas it showed a smooth surface on the (111)A patterned substrate (Figure 4 in Paper I). Figure 12 compares the (112)A sidewall layers on the (111)A and (001) patterned substrates, as an example of this difference. This may be attributed to the difference in the effective beam fluxes and flux ratio due to the difference in θ for the (112)A sidewall between the two substrates and/or the difference in the Ga surface diffusion process between the combinations of the (112)A sidewall - (111)A substrate plane without extra facets and the (112)A sidewall - (114)A facet - (001) substrate plane.

We would like to emphasize that the above considerations have led to the successful fabrication of lateral p-n junctions [9-11] and lateral p-n subband junctions [61], both with a $[\bar{1}\bar{1}2]$A interface, on a (111)A substrate - (113)A sidewall configuration.

(2) Systems including the $(\bar{1}\bar{1}\bar{1})$B surface

The $(\bar{1}11)$B facet generating on the [110] stripe with an inverted mesa on (001) substrates has been reported in several papers [18, 24, 25]. The $(\bar{1}\bar{1}\bar{1})$B facet with low growth rates was used for fabricating edge quantum wires in combination with special molecular beam arrangements [24]. A flat (001) surface and an enhanced growth rate in the [001] direction were realized by reducing the width of the upper (001) substrate plane of the stripe to the order of $\lambda_{Ga}(001)$. For (111)A patterned substrates, since the growth rate of the $(11\bar{1})$B facet was enhanced by the lateral Ga atom migration from the adjacent (111)A substrate plane, fabrication of edge quantum wires may be more difficult. In addition, the θ for which the $(11\bar{1})$B facet exists is limited to a narrow region larger than 71 ° and the (110) facet irregularly generates together with the $(11\bar{1})$B facet along the [110] direction (see Figure 11(b)). Consequently, the (001) patterned substrate is preferable to the (111)A patterned substrate in using the $(\bar{1}\bar{1}\bar{1})$B facet for this particular purpose.

(3) Systems including the (110) surface

Facet generation on the [100] stripe on (001) substrates has not been studied to date. Only recently has growth of the (011) facet on the [100] stripe been studied and have new quantum wires surrounded by two equivalent (110) facets intersecting at right angles and the (001) substrate plane been formed by growing GaAs/AlAs multilayers under similar growth conditions as ours [28]. An extremely low R' of the (110) facet shown in Table 1 and the excess Ga atom migration to the (001) substrate plane discussed in an earlier section was also reported in [28]. Considering that their quantum wires are based on the inequality of $\lambda_{Ga}(001) < \lambda_{Ga}(110)$ and the two-fold rotational symmetry of the (001) surface, new quantum dots, surrounded by three equivalent (110) facets and the (111)A substrate plane or three equivalent (113)A facets, can be formed on the (110) triangle in a similar way on the basis of the inequality of $\lambda_{Ga}(113)A < \lambda_{Ga}(111)A \leqq \lambda_{Ga}(110)$, the three-fold rotational symmetry of the (111)A surface, and no generation of extra facets on the triangle corners. Since flat (111)A layers can be grown with three equivalent $(\bar{1}01)$ edges on the (201) triangles with inverted mesa sidewalls on the basis of the inequality of $\lambda_{Ga}(111)A \leqq \lambda_{Ga}(110)$, other new quantum dots can be obtained on the (201) triangle (and also on the (021) triangle). As a modification, quantum wires can be formed on stripes running in the $[\bar{1}\bar{1}2]$A direction on (111)A substrates on the same mechanism, as easily understood from the equivalency of the (201) and (021) triangles (see Figure 1 in Paper I).

3. Comments on $(\bar{1}\bar{1}\bar{1})$B and (110) patterned substrates

Based on the orientation dependence of λ_{Ga} obtained in this study, some comments can be made on growth on $(\bar{1}\bar{1}\bar{1})$B and (110) patterned substrates in addition to the (001) and (111)A patterned substrates discussed above.

(1) $(\bar{1}\bar{1}\bar{1})$B patterned substrates

Growth behavior on the $[\bar{1}10]$ stripes on $(\bar{1}\bar{1}\bar{1})$B substrates has been studied in metalorganic MBE (MOMBE) in [26, 27]. Taking advantage of the properties specific to the $(\bar{1}\bar{1}\bar{1})$B surface that the growth rate on the $(\bar{1}\bar{1}\bar{1})$B surface is suppressed as the As_4 pressure increases due to the formation of growth-

hampering As trimers on the $(\bar{1}\bar{1}\bar{1})$B surface [31-33], GaAs layers have been successfully grown only on the exposed $(\bar{2}\bar{2}1)$A and $(00\bar{1})$ sidewalls with the generation of extra $(\bar{1}\bar{1}0)$ and $(\bar{1}\bar{1}\bar{3})$B facets, respectively, under high As_4 pressures.

Next, consider the growth under ordinary MBE growth conditions on the basis of the orientation dependence of λ_{Ga} obtained in this study. In [62], we have described the selective etching characteristics of $HF+H_2O_2+H_2O$ mixtures on the $(\bar{1}\bar{1}\bar{1})$B surface. The $(00\bar{1})$, $(\bar{1}\bar{1}0)$, and $(\bar{2}0\bar{1})$ triangles can be formed on $(\bar{1}\bar{1}\bar{1})$B substrates with the $HF+H_2O_2+H_2O$ mixtures in the same manner as on (111)A substrates, although the $(\bar{1}\bar{1}0)$ triangle is really a hexagon due to the etching anisotropy. For the $(00\bar{1})$ triangles, with the $(\bar{1}\bar{1}\bar{N})$B sidewalls, flat layers will be obtained on the $(\bar{1}\bar{1}\bar{1})$B substrate plane and exponential thickness variations will appear for the $(\bar{1}\bar{1}\bar{N})$B sidewall layers towards the boundary with extra facets possibly generating during growth. The extra facets expected from the present study will be $(\bar{1}\bar{1}\bar{3})$B on the sidewall and $(\bar{1}\bar{1}0)$ on the corner. For the $(\bar{1}\bar{1}0)$ triangles, with $(\bar{1}\bar{1}1)$A, $(\bar{N}\bar{N}1)$A, $(\bar{1}\bar{1}0)$, and $(\bar{N}\bar{N}\bar{1})$B sidewalls depending on θ, an exponential thickness variation will always appear for the layers on the $(\bar{1}\bar{1}\bar{1})$B substrate plane towards the boundary with extra facets possibly generating during growth. The extra facets expected from the present study will be $(\bar{1}\bar{1}0)$ and $(\bar{1}\bar{1}3)$A. Considering the orientation-dependent Si doping characteristics and the actual shape of the $(\bar{1}\bar{1}0)$ triangle, carrier confinement structures cannot be formed on either the $(00\bar{1})$ or $(\bar{1}\bar{1}0)$ triangle by growing Si-doped GaAs on it. Lateral p-n junctions, however, can be fabricated on the $(\bar{1}\bar{1}1)$A, $(\bar{N}\bar{N}1)$A, and $(\bar{1}\bar{1}0)$ sidewalls of stripes running in the $[\bar{1}10]$ direction. The growth properties specific to the $(\bar{1}\bar{1}\bar{1})$B surface mentioned above, of course, may change the expected growth profile depending on the growth conditions, especially the As_4 pressure.

(2) (110) patterned substrates

There have been no reports on the growth on (110) patterned substrates to our knowledge. In [62], we have also described the selective etching characteristics of

$HF+H_2O_2+H_2O$ mixtures on the (110) surface. The $HF+H_2O_2+H_2O$ mixtures of various compositions can produce stripes running in the $[\bar{1}10]$ direction with the (NN1)A sidewall on one side and the (NN$\bar{1}$)B sidewall on the opposite side. Since $\lambda_{Ga}(110)$ is the longest, flat layers can always be grown on the (110) substrate plane as they can on the (111)A patterned substrate, while any exponential thickness variation will appear for the sidewall layers towards the boundary with extra facets possibly generating during growth. Extra (221)A and/or (113)A facets are expected to generate on the (NN1)A sidewall while no particular facets are expected on the (NN$\bar{1}$)B sidewall. Considering the orientation-dependent Si doping characteristics, lateral p-n junctions can be fabricated on the (NN$\bar{1}$)B sidewall but cannot be fabricated on the (NN1)A sidewall by growing Si-doped GaAs on the $[\bar{1}10]$ stripe.

4. Summary and Conclusion

Extra facet generation on ridge-type triangles with (001)-, (110)-, and (201)-related equivalent slopes on GaAs (111)A substrates and stripes running in the $[\bar{1}10]$, [110], and [100] directions on (001) substrates during molecular beam epitaxy of GaAs/AlGaAs multilayers has been studied. By investigating the local variation in layer thickness in the regions adjacent to the facets common to the (111)A and (001) patterned substrates and extra facets specific to the respective substrates together with the relative growth rates of the facets, the orientation-dependent Ga surface diffusion length, λ_{Ga}, has been elucidated as $\lambda_{Ga}(001) \approx \lambda_{Ga}(\bar{1}\bar{1}\bar{3})B < \{\lambda_{Ga}(\bar{1}\bar{1}\bar{1})B, \lambda_{Ga}(\bar{3}\bar{3}\bar{1})B, \lambda_{Ga}(013), \lambda_{Ga}(113)A\} < \lambda_{Ga}(159) \approx \lambda_{Ga}(114)A \approx \lambda_{Ga}(111)A \leqq \lambda_{Ga}(110)$. Several bulk and epitaxial growth processes and amphoteric doping properties of Si impurity were also discussed in connection with the orientation dependence of λ_{Ga}.

From the point of view of device application, the merits and demerits of the (001) and (111)A patterned substrates were compared on the basis of this inequality. In this respect, the following was pointed out: The present result that $\lambda_{Ga}(001)$ is the shortest may limit the use of (001) patterned substrates for the

fabrication of lateral p-n junctions because an exponential variation of the layer thickness always appears on the (001) substrate plane at the boundary with the sidewall and hampers the formation of simple structures. In contrast, (111)A and (110) substrates with relatively long λ_{Ga} are free from such a limitation, and hence may be more suitable for device application, although epitaxial growth of good layers on (111)A and (110) surfaces is very difficult. On the other hand, the (001) substrate will be suitable for the formation of quantum wires and dots on patterns with dimensions around λ_{Ga} because the preferential incorporation of Ga adatoms into the (001) surface leads to enhancement of the growth rate in the (001) direction and suppression of the growth rates in the other directions.

-ACKNOWLEDGMENTS-

The authors would like to thank Dr. Y. Furuhama for his encouragement throughout this work. The authors also would like to thank Prof. S. Hiyamizu, Dr. S. Shimomura, and Dr. Y. Liu of Osaka University for invaluable discussions.

-APPENDIX-

In this appendix, we present a procedure for evaluating the actual intersection angle, θ_f, of a facet to the substrate plane, the actual angle, θ_g, of the facet growth direction to the substrate orientation, and the actual growth thickness, l, of the facet from the corresponding apparent values, θ_f', θ_g', and l', mesured on the SEM cross-sectional image when the cleavage plane for the cross-sectional observation is not at right angles to the sidewall in question, but misoriented by θ_m. For the (021) triangle on the (111)A substrate, $\theta_m=30°$, for the [100] stripe on the (001) substrate, $\theta_m=45°$, and for the other patterns, $\theta_m=0°$.

Since the growth direction of a facet is normal to the facet plane in the actual space by definition, the equality

$$\theta_g=\theta_f \qquad (1)$$

always holds. In the image, in general, $\theta_g'\neq\theta_f'$. By simple geometrical considerations and calculations, we have following relations.

$\theta_f = \tan^{-1}(\tan\theta_f'/\cos\theta_m)$ (2)

$\theta_g' = \tan^{-1}(\tan\theta_f'/\cos^2\theta_m)$ (3)

$l = l'\cos\theta_g'/\cos\theta_f$ (4)

Thus, we can obtain the values of θ_f, θ_g', and l from θ_f', θ_m, and l'. For $\theta_m = 0°$, $\theta_f = \theta_g = \theta_g' = \theta_f'$ and $l = l'$ hold as a matter of course. For $\theta_f = 0°$, that is, the growth on the substrate plane, $\theta_f' = \theta_g' = 0°$ and $l' = l$ hold, implying that the actual values are read directly from the image. For $\theta_f = 90°$, that is, the growth of a facet vertical to the substrate plane, $\theta_f' = \theta_g' = 90°$ holds, implying that the facet is vertical to the substrate plane also on the image. Since $\cos\theta_f = 0$, equation (4) cannot be used to evaluate l from l' and a further modification to the equation is required. That is, for $\theta_f \to 90°$, since $\sin\theta_f \to 1$, $\tan\theta_f \to \cos^{-1}\theta_f$ holds. Likewise, $\tan\theta_f' \to \cos^{-1}\theta_f'$ and $\tan\theta_g' \to \cos^{-1}\theta_g'$ hold. Therefore, a transformation $\cos\theta_g'/\cos\theta_f \to \tan\theta_f/\tan\theta_g' = (\tan\theta_f'/\cos\theta_m)/(\tan\theta_f'/\cos^2\theta_m)$ (from (2) and (3)) $= \cos\theta_m$ results. Consequently, Equation (4) reduces to

$l = l'\cos\theta_m$ (for $\theta_f = 90°$), (4')

which can be understood by intuition.

If d is the thickness of the layer grown on the substrate plane and l[lmn] that of an (lmn) facet in the same period of time, then, the relative growth rate, R'[lmn], of the facet is expressed as

R'[lmn] = l[lmn]/d. (5)

-REFERENCES-

[1] D. L. Miller, Appl. Phys. Lett. **47**, 1309 (1985).

[2] D. L. Miller and P. M. Asbeck, J. Crystal Growth 81, 368 (1987).

[3] H. P. Meier, R. F. Broom, P. W. Epperlein, E. van Gieson, Ch. Harder, H. Jäckel, W. Walter, and D. J. Webb, J. Vac. Sci. Technol. B **6**, 692 (1987).

[4] H. P. Meier, E. van Gieson, R. F. Broom, W. Walter, D. J. Webb, C. Harder, and H. Jäckel, Inst. Phys. Conf. Ser. No.**91**, 609 (1988).

[5] E. Kapon, J. P. Harbison, C. P. Yun, and N. G. Stoffel, Appl. Phys. Lett. **52**, 607 (1988).

[6] H. Jäckel, H. P. Meier, G. L. Bona, W. Walter, D. J. Webb, and E. van Gieson, Appl. Phys. Lett. **55**, 1059 (1989).

[7] T. Takamori, K. Watanabe, and T. Kamijo, Electron. Lett. 28, 1419 (1992).

[8] T. Takamori, Y. K. Sin, K. Watanabe, and T. Kamijo, Appl. Phys. Lett. **61**, 2266 (1992).

[9] M. Fujii, T. Yamamoto, M. Shigeta, T. Takebe, K. Kobayashi, S. Hiyamizu, and I. Fujimoto, Surf. Sci. **267**, 26 (1992).

[10] M. Fujii, T. Takebe, T. Yamamoto, M. Inai, and K. Kobayashi, Superlattices and Microstructures **12**, 167 (1992).

[11] K. Kobayashi, T. Takebe, T. Yamamoto, M. Fujii, M. Inai, and D. Lovell, J. Electron. Mat. **22**, 161 (1993).

[12] K. Inoue, K. Kimura, K. Maehashi, S. Hasegawa, and H. Nakashima, J. Crystal Growth **127**, 1041 (1993).

[13] M. Hata, T. Isu. A. Watanabe, and Y. Katayama, Appl. Phys. Lett. **56**, 2542 (1990).

[14] M. Hata, T. Isu. A. Watanabe, and Y. Katayama, J. Vac. Sci. Technol. B 8, 692 (1990).

[15] X. Q. Shen, M. Tanaka, and T. Nishinaga, 10th Symp. Rec. Alloy Semicond. Phys. Electron. 65 (1991).

[16] X. Q. Shen and T. Nishinaga, 12th Symp. Rec. Alloy Semicond. Phys. Electron. 367 (1993).

[17] X. Q. Shen and T. Nishinaga, Jpn. J. Appl. Phys. **32**, L1117 (1993).

[18] W. T. Tsang and A. Y. Cho, Appl. Phys. Lett. **30**, 293 (1977).

[19] J. S. Smith, P. L. Derry, S. Margalit, and A. Yariv, Appl. Phys. Lett. **47**, 712 (1985).

[20] T. Yuasa, M. Manno, T. Yamada, S. Narituka, K. Shinozaki, and M. Ishii, J. Appl. Phys. **62**, 764 (1987).

[21] E. Kapon, M. C. Tamargo, and D. M. Hwang, Appl. Phys. Lett. **50**, 347 (1987).

[22] S. Shimomura, S. Ohkubo, Y. Yuba, S. Namba, S. Hiyamizu, M. Shigeta, T. Yamamoto, and K. Kobayashi, Surf. Sci. **267**, 13 (1992).

[23] X. Q. Shen, M. Tanaka, and T. Nishinaga, 11th Symp. Rec. Alloy Semicond. Phys. Electron. 333 (1992).

[24] Y. Nakamura, S. Koshiba, M. Tsuchiya, H. Kano, and H. Sakaki, Appl. Phys. Lett. **59**, 700 (1991).

[25] M. Walther, T. Röhr, G. Böhm, G. Tränkle, and G. Weimann, J. Crystal Growth **127**, 1045 (1993).

[26] Y. Nomura, Y. Morishita, S. Goto, Y. Katayama, and T. Isu, Jpn. J. Appl. Phys. **30**, 3771 (1991).

[27] T. Isu, Y. Morishita, S. Goto, Y. Nomura, and Y. Katayama, J. Crystal Growth **127**, 942 (1993).

[28] M. López, T. Ishikawa, and Y. Nomura, Jpn. J. Appl. Phys. **32**, L1051 (1993).

[29] K. Tsutsui, H. Mizukami, O. Ishiyama, S. Nakamura, and S. Furukawa, Jpn. J. Appl. Phys. **29**, 468 (1990).

[30] P. Chen, K. C. Rajkumar, and A. Madhukar, Appl. Phys. Lett. **58**, 1771 (1991).

[31] T. Hayakawa, M. Nagai, M. Morishima, H. Horie, and K. Matsumoto, Appl. Phys. Lett. **59**, 2287 (1991).

[32] T. Hayakawa, M. Morishima, and S. Chen, Appl. Phys. Lett. 59, 3321 (1991).

[33] T. Hayakawa, M. Morishima, M. Nagai, H. Horie, and K. Matsumoto, Surf. Sci. **267**, 8 (1992).

[34] J. Fu, K. Zhang, and D. L. Miller, J. Vac. Sci. Technol. B **10**, 779 (1992).

[35] D. A. Woolf, Z. Sobiesierski, D. I. Westwood, and R. H. Williams, J. Appl. Phys. **71**, 4908 (1992).

[36] W. I. Wang, J. Vac. Sci. Technol. B **1**, 630 (1983).

[37] L. T. Parechanian, E. R. Weber, T. L. Hierl, Mat. Res. Soc. Symp. Proc. **46**, 391 (1985).

[38] Z. Junming, H. Yi, L. Yongkang, and J. W. Yi, J. Crystal Growth **81**, 221 (1987).

[39] L. Pfeiffer, K. W. West, H. L. Stromer, J. P. Eizenstein, K. W. Baldwin, D. Gershoni, and J. Spector, Appl. Phys. Lett. **56**, 1697 (1990).

[40] G. Tanaka, K. Hirakawa, H. Ichinose, and T. Ikoma, Inst. Phys. Conf. Ser. No.**120**, 25 (1992).

[41] Y. Okano, M. Shigeta, H. Seto, H. Katahama, S. Nishine, and I. Fujimoto, Jpn. J. Appl. Phys. **29**, L1357 (1990).

[42] S. Fuke, M. Umemura, N. Yamada, K. Kuwahara, and T. Imai, J. Appl. Phys. **68**, 97 (1990).

[43] M. Umemura, K. Kuwahara, S. Fuke, M. Sato, and T. Imai, J. Appl. Phys. **72**, 313 (1992).

[44] A. Y. Cho, M. B. Panish, and I. Hayashi, Inst. Phys. Conf. Ser. No.**9**, 18 (1970).

[45] J. M. Ballingall and C. E. C. Wood, Appl. Phys. Lett. **41**, 947 (1982).

[46] Y. Okano, H. Seto, H. Katahama, S. Nishine, I. Fujimoto, and T. Suzuki, Jpn. J. Appl. Phys. **28**, L151 (1989).

[47] Y. Kadoya, A. Sato, H. Kano, and H. Sakaki, J. Crystal Growth **111**, 280 (1991).

[48] M. Shigeta, Y. Okano, H. Seto, H. Katahama, S. Nishine, K. Kobayashi, and I. Fujimoto, J. Crystal Growth **111**, 284 (1991).

[49] M. R. Fahy, J. H. Neave, M. J. Ashwin, R. Murray, R. C. Newman, B. A. Joyce, Y. Kadoya, and H. Sakaki, J. Crystal Growth **127**, 871 (1993).

[50] D. A. Woolf, J. P. Williams, D. I. Westwood, Z. Sobiesierski, J. E. Aubrey, and R. H. Williams, J. Crystal Growth **127**, 913 (1993).

[51] P. N. Uppal, J. S. Ahearn, and D. P. Musser, J. Appl. Phys. **62**, 3766 (1987).

[52] W. I. Wang, E. E. Mendez, T. S. Kuan, and L. Esaki, Appl. Phys. Lett. **47**, 826 (1985).

[53] W. I. Wang, E. E. Mendez, Y. Iye, B. Lee, M. H. Kim, and G. E. Stillman, J. Appl. Phys. **60**, 1834 (1986).

[54] S. Subbanna, H. Kroemer, and J. L. Merz, J. Appl. Phys. **59**, 488 (1986).

[55] T. Takamori, T. Fukunaga, J. Kobayashi, K. Ishida, and H. Nakashima, Jpn. J. Appl. Phys. **26**, 1097 (1987).

[56] S. S. Bose, B. Lee, M. H. Kim, G. E. Stillman, and W. I. Wang, J. Appl. Phys. **63**, 743 (1988).

[57] T. Takamori, K. Watanabe, and T. Fukunaga, Electron. Lett. **27**, 729 (1991).

[58] W. Q. Li, P. K. Bhattacharya, S. H. Kwok, and R. Merlin, J. Appl. Phys. **72**, 3129 (1992).

[59] A. Chin, P. Martin, P. Ho, J. Ballingall, T. -H. Yu, and J. Mazurowski, Appl. Phys. Lett. **59**, 1899 (1991).

[60] H. Imamoto, F. Sato, K. Imanaka, and M. Shimura, Appl. Phys. Lett. **55**, 115 (1989).

[61] T. Yamamoto, M. Inai, T. Takebe, and T. Watanabe, Jpn. J. Appl. Phys. **32**, L28 (1993).

[62] T. Takebe, T. Yamamoto, M. Fujii, and K. Kobayashi, J. Electrochem. Soc. **140**, 1169 (1993).

-FIGURE CAPTIONS-

Figure 1 Extra (114)A, (110), and $(\bar{1}\bar{1}\bar{1})$B facets common to the (111)A and (001) patterned substrates.

Figure 2 Cross-sectional profiles of (a) the (111)A sidewall of the $[\bar{1}10]$ stripe and (b) the (001) sidewall of the (001) triangle.

Figure 3 Cross-sectional profiles of (a) the upper and (b) lower parts of the $(\bar{2}\bar{2}5)$A sidewall of the (001) triangle.

Figure 4 A top view of the (119)A facet on the intersection of the [100] and [010] stripes.

Figure 5 Cross-sectional profiles of (a) the (445)A and (b) (335)A sidewalls of the $[\bar{1}10]$ stripes.

Figure 6 Cross-sectional profiles of (a) the (010) sidewall of the [100] stripe, (b) the $(33\bar{1})$B sidewall of the (110) triangle, and (c) the $(\bar{2}14)$ sidewall with an inverted mesa of the (210) triangle.

Figure 7 Top views of the corners of (a) the (001) triangle with the (001) sidewalls ($\theta = 54°$) and (b) the (021) triangle with the $(\bar{2}38)$ sidewalls ($\theta = 55°$).

Figure 8 Cross-sectional profiles of (a) the $(\bar{1}11)$B sidewall with an inverted mesa of the [110] stripe and (b) the $(77\bar{8})$B sidewall of the (110) triangle.

Figure 9 A cross-sectional profile of the $(\bar{1}12)$B sidewall of the [110] stripe.

Figure 10 A cross-sectional profile of the (045) sidewall of the [100] stripe.

Figure 11 A cross-sectional profile of the $(\bar{3}27)$ sidewall of the (201) triangle.

Figure 12 Bird's eye views of the (112)A sidewall layers (indicated by arrow) on (a) the (111)A and (b) (001) patterned substrates.

-TABLE HEADINGS-

Table 1 summary of relative growth rates of the facets.

Table 2 summary of orientation dependences of the Ga surface diffusion length.

(111)A patterned substrates ↓ | (001) patterned substrates ↓

(a) (110) facet $\theta_f = 35°$ | $\theta_f = 45°$

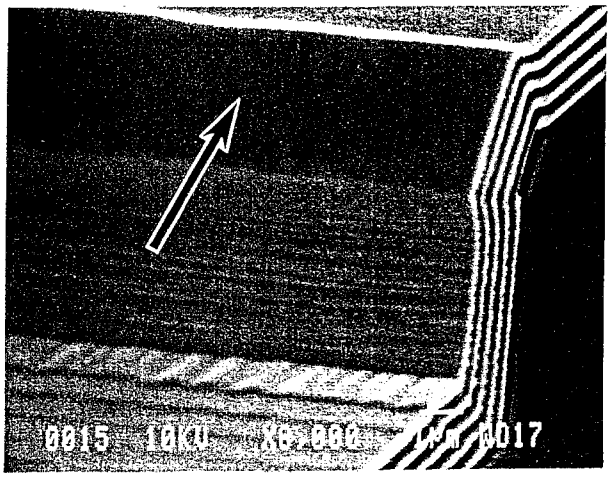

"(110) triangle / $\theta = 49°$"

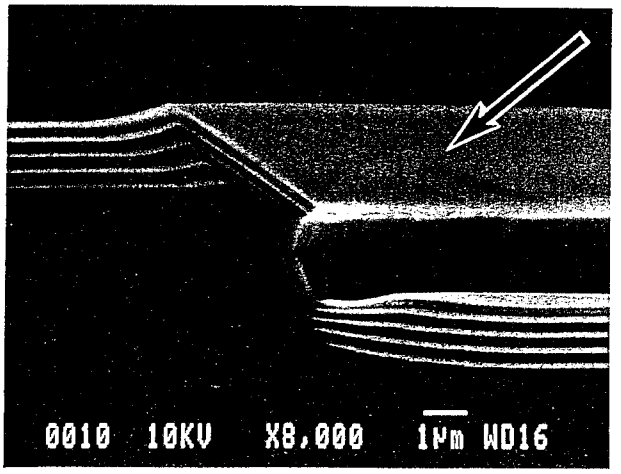

"[100] stripe / $\theta = 89°$"

(b) (114)A facet $\theta_f = 33°$ | $\theta_f = 21°$

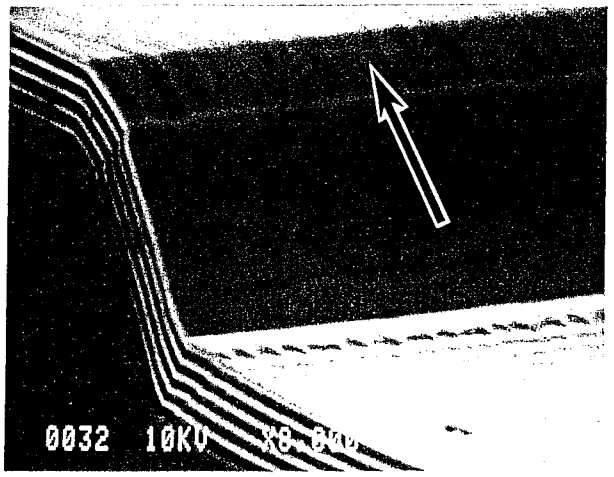

"(001) triangle / $\theta = 52°$"

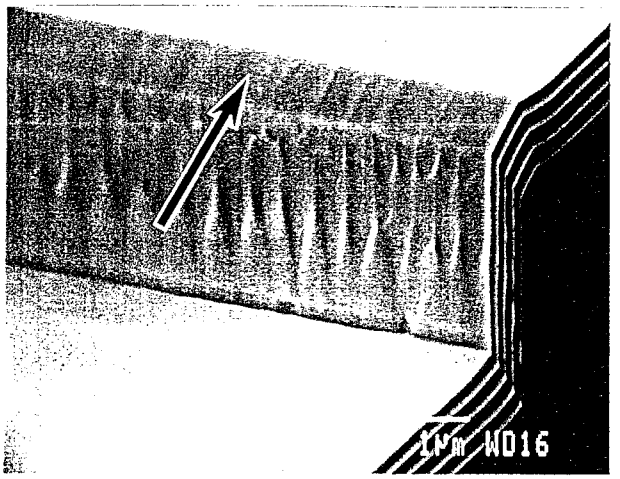

"[$\bar{1}$10] stripe / $\theta = 54°$"

(c) ($\bar{1}\bar{1}\bar{1}$)B facet $\theta_f = 71°$ | $\theta_f = 53°$

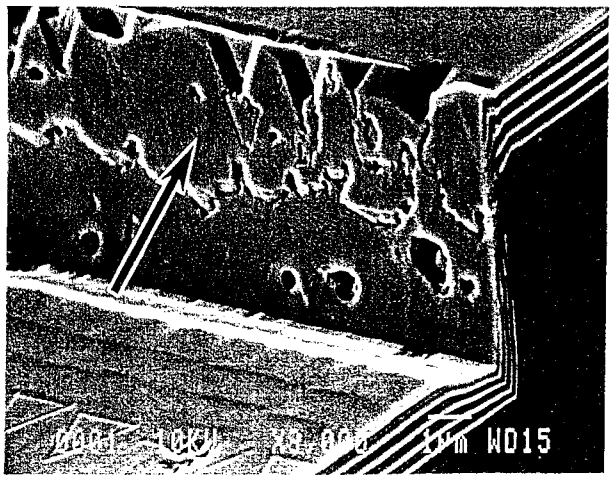

"(110) triangle / $\theta = 74°$"

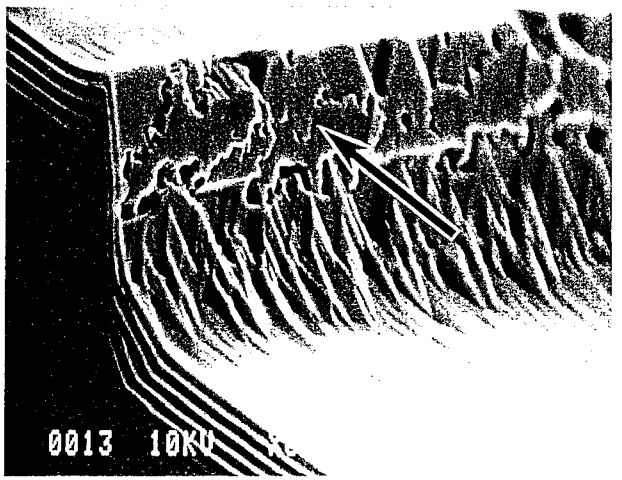

"[110] stripe / $\theta = 52°$"

Figure 1 Extra (114)A, (110), and ($\bar{1}\bar{1}\bar{1}$)B facets common to the (111)A and (001) patterned substrates.

(114)A facet

(a) (114)A / θ_f = 21°

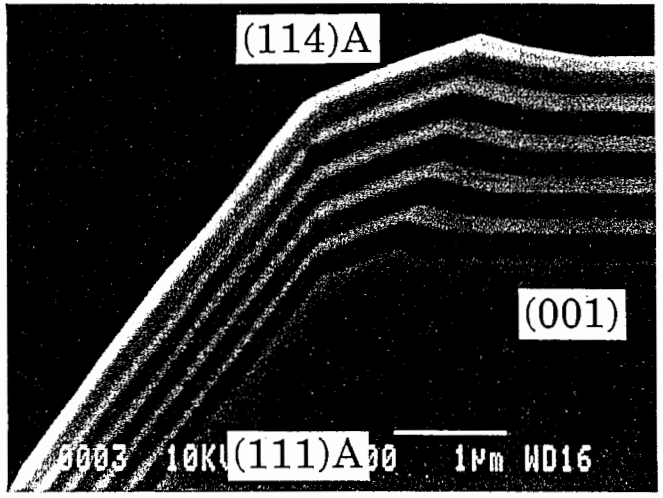

"[$\bar{1}$10] stripe : θ = 54° / (111)A"

(b) (114)A / θ_f = 33°

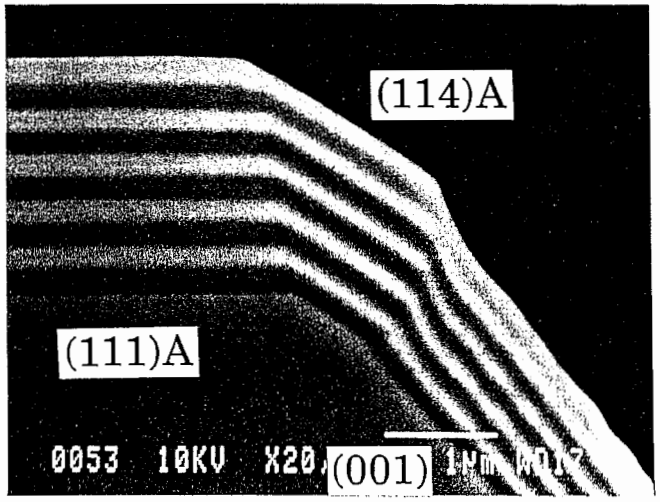

"(001) triangle : θ = 54° / (001)"

Figure 2 Cross-sectional profiles of (a) the (111)A sidewall of the [$\bar{1}$10] stripe and (b) the (001) sidewall of the (001) triangle.

(113)A facet

(a) $(\bar{1}\bar{1}3)$A / θ_f = 80°

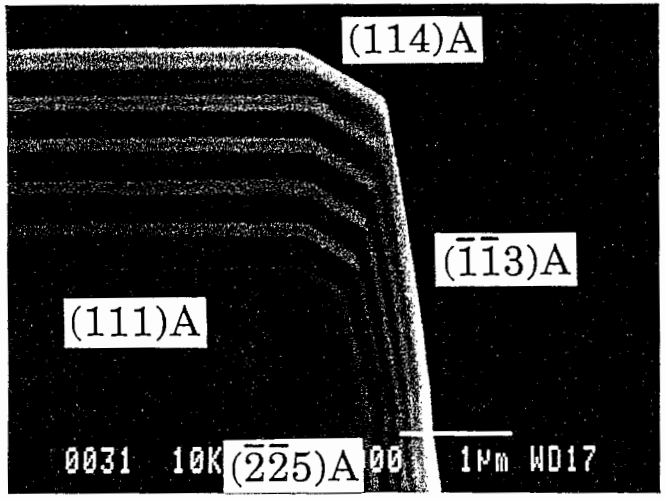

"(001) triangle : θ = 84° / $(\bar{2}\bar{2}5)$A"

(001) facet

(b) (001) / θ_f = 55°

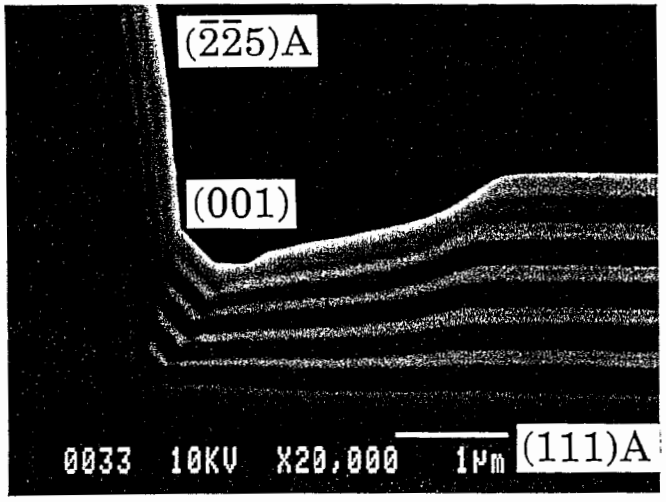

"(001) triangle : θ = 84° / $(\bar{2}\bar{2}5)$A"

Figure 3 Cross-sectional profiles of (a) the upper and (b) lower parts of the $(\bar{2}\bar{2}5)$A sidewall of the (001) triangle.

(119)A facet

(119)A / θ_f = 9°

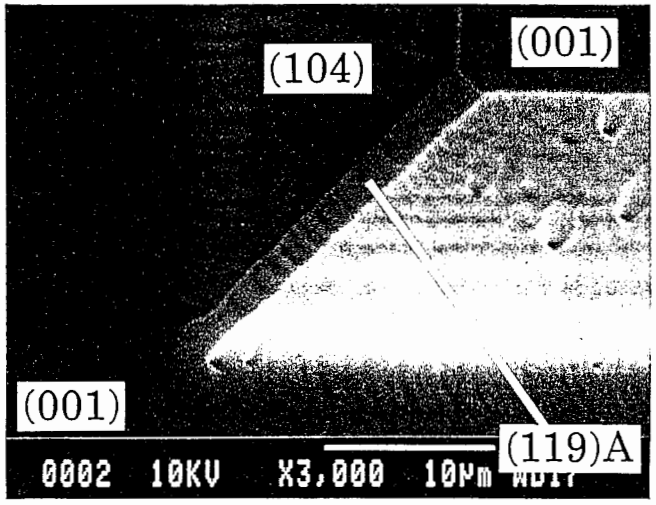

"[100] and [010] stripes : θ = 13° / (104)"

Figure 4 A top view of the (119)A facet on the intersection of the [100] and [010] stripes.

(111)A facet

(a) (111)A / θ_f = 55°

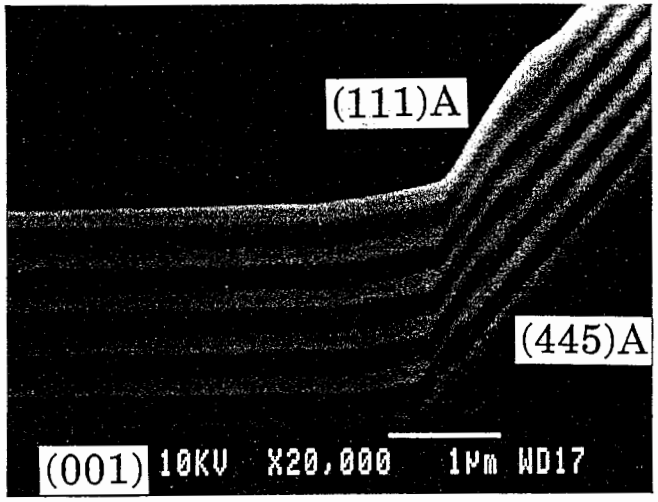

"[$\bar{1}$10] stripe : θ = 48° / (445)A"

(b) (111)A / θ_f = 55°

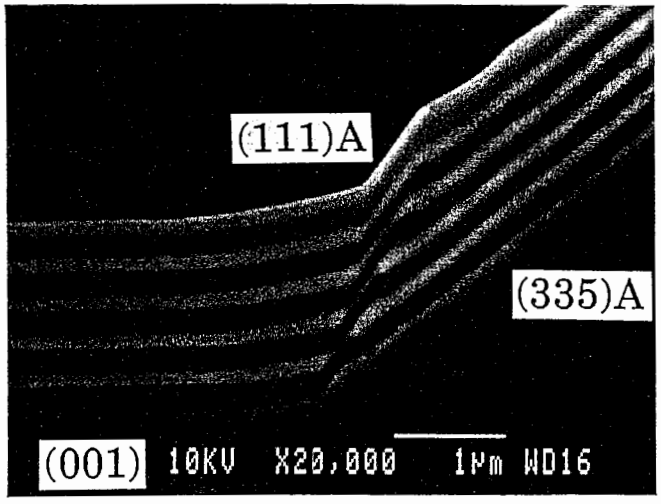

"[$\bar{1}$10] stripe : θ = 41° / (335)A"

Figure 5 Cross-sectional profiles of (a) the (445)A and (b) (335)A sidewalls of the [$\bar{1}$10] stripes.

(110) facet

(a) (011) / θ_f = 45°

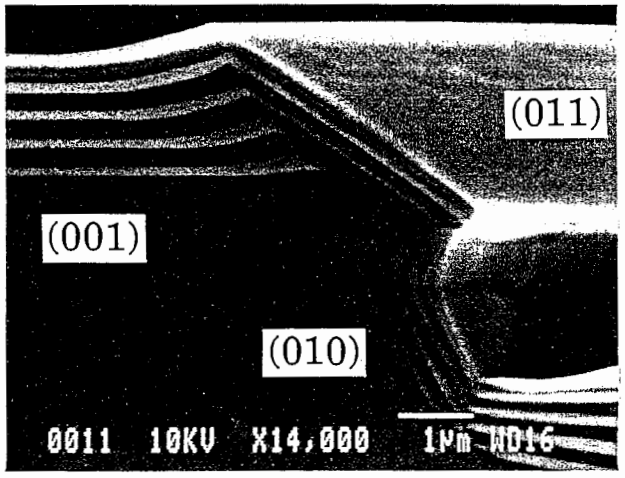

"[100] stripe : θ = 89° / (010)"

(b) (110) / θ_f = 35°

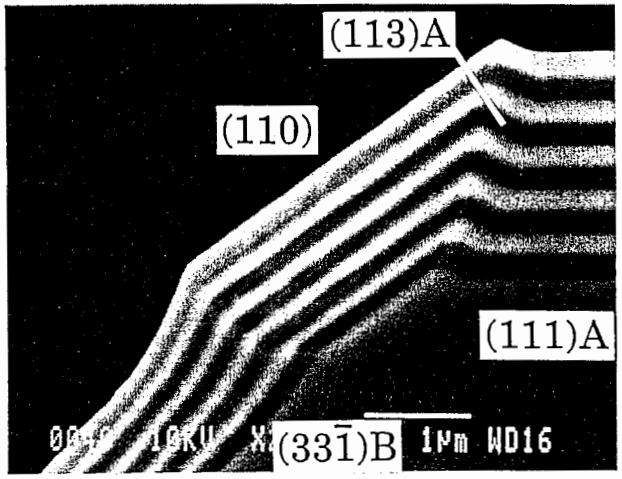

"(110) triangle : θ = 49° / (33$\bar{1}$)B"

(c) ($\bar{1}$01) / θ_f = 90°

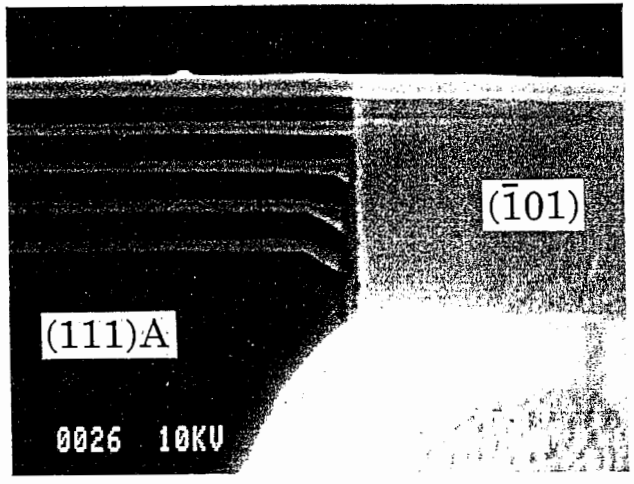

"(201) triangle : θ = 69° / ($\bar{2}$14)"

Figure 6 Cross-sectional profiles of (a) the (010) sidewall of the [100] stripe, (b) the (33$\bar{1}$)B sidewall of the (110) triangle, and (c) the ($\bar{2}$14) sidewall with an inverted mesa of the (210) triangle.

<u>(110) facet</u>

(a) (110) / θ_f = 35 °

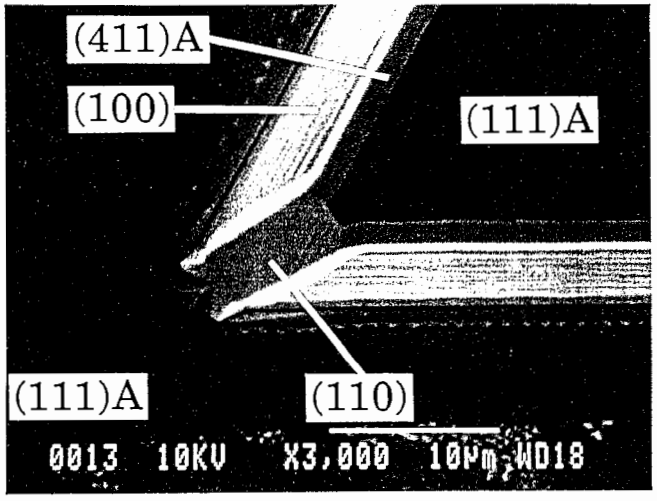

"(001) triangle : θ = 54 ° / (100)"

(b) (110) / θ_f = 35 °

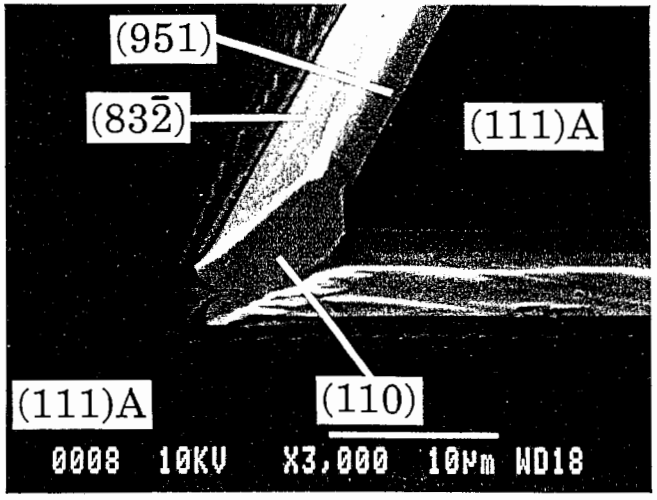

"(021) triangle : θ = 55 ° / (83$\bar{2}$)"

Figure 7 Top views of the corners of (a) the (001) triangle with the (001) sidewalls (θ=54 °) and (b) the (021) triangle with the ($\bar{2}$38) sidewalls (θ=55 °).

$(\bar{1}\bar{1}\bar{1})$B facet

(a) $(\bar{1}11)$B / θ_f = 53 °

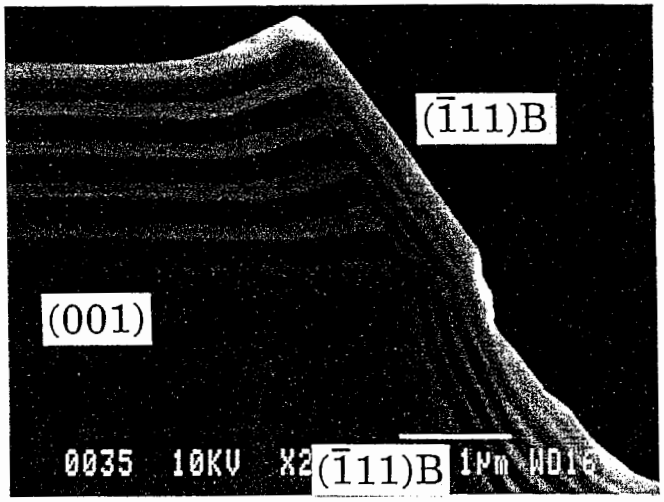

"[110] stripe : θ = 54 ° / $(\bar{1}11)$B"

(b) $(11\bar{1})$B / θ_f = 71 °

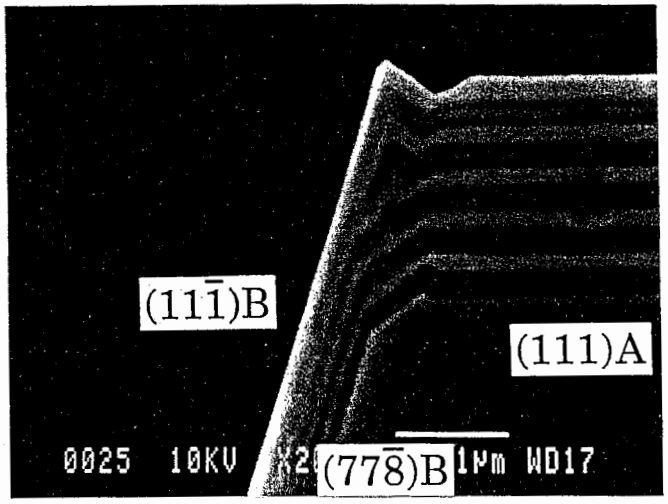

"(110) triangle : θ = 74 ° / $(77\bar{8})$B"

Figure 8 Cross-sectional profiles of (a) the $(\bar{1}11)$B sidewall with an inverted mesa of the [110] stripe and (b) the $(77\bar{8})$B sidewall of the (110) triangle.

$(\bar{1}\bar{1}\bar{3})$B facet

$(\bar{1}13)$B / θ_f = 24°

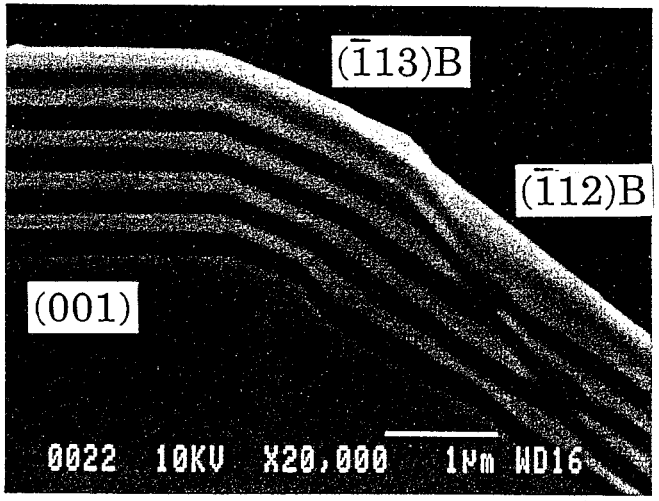

"[110] stripe : θ = 36° / $(\bar{1}12)$B"

Figure 9 A cross-sectional profile of the $(\bar{1}12)$B sidewall of the [110] stripe.

(013) facet

(013) / θ_f = 19 °

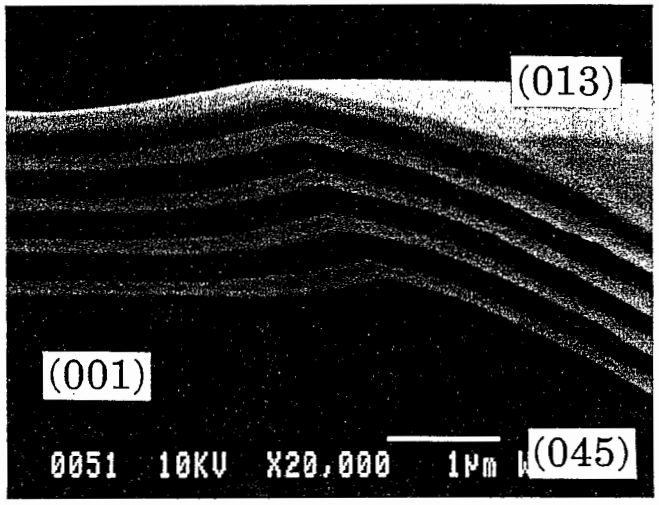

"[100] stripe : θ = 39 ° / (045)"

Figure 10 A cross-sectional profile of the (045) sidewall of the [100] stripe.

(159) facet

(159) / θ_f = 34 °

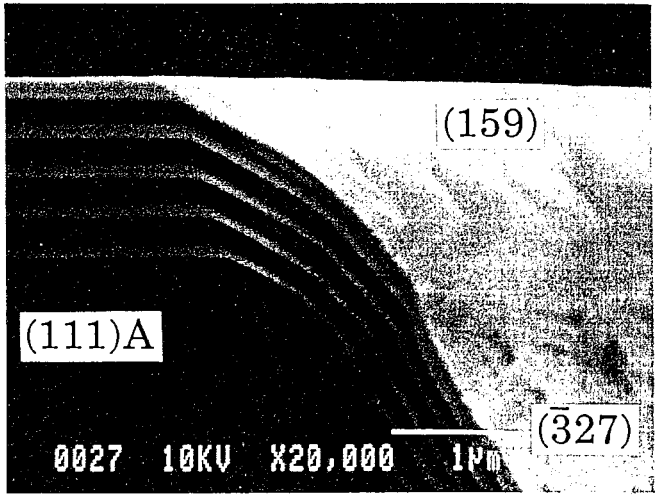

"(201) triangle : θ = 63 ° / (3̄27)"

Figure 11 A cross-sectional profile of the (3̄27) sidewall of the (201) triangle.

(a) "(111)A substrate / (001) triangle" : θ = 20 ° / (112)A

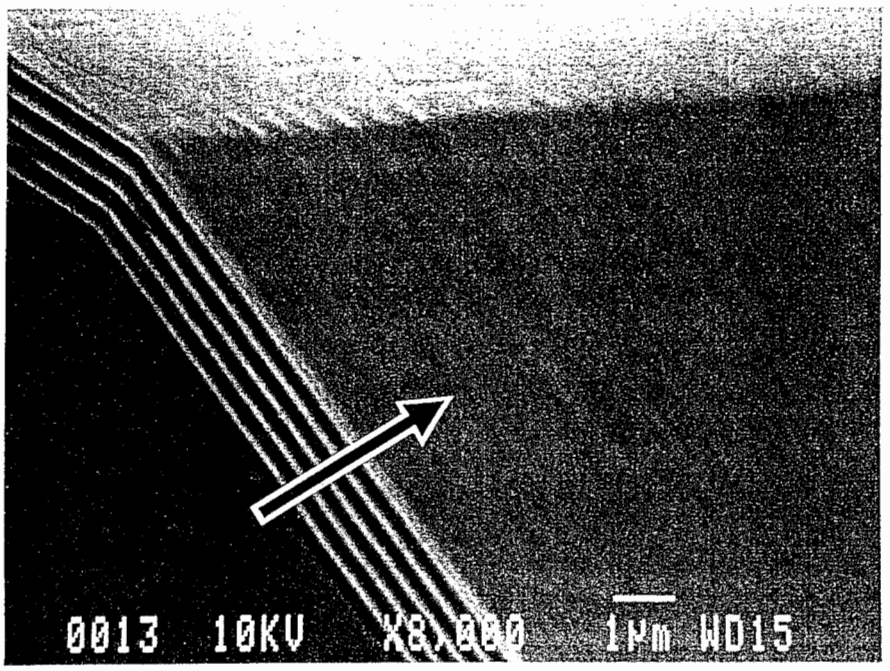

(b) "(001) substrate / [$\bar{1}$10] stripe" : θ = 37 ° / (112)A

Figure 12 Bird's eye views of the (112)A sidewall layers (indicated by arrow) on (a) the (111)A and (b) (001) patterned substrates.

Facet	Substrate	θ_f	R'[lmn]	R''[lmn]	R' / R''
(114)A	(111)A	33 °	0.81	0.84	0.96
	(001)	21 °	0.86	0.93	0.92
(011)	(001)	45 °	0.47	0.71	0.67
(110)	(111)A	35 °	0.73	0.82	0.89
($\bar{1}$01)		90 °	0.12	0.00	——
(11$\bar{1}$)B	(111)A	71 °	0.37	0.33	1.13
($\bar{1}$11)B	(001)	53 °	0.46	0.60	0.77
(001)	(111)A	55 °	0.62	0.57	1.09
(113)A	(111)A	30 °	1.05	0.86	1.22
($\bar{1}\bar{1}$3)A		80 °	0.33	0.17	1.91
(159)	(111)A	34 °	0.85	0.83	1.02
			0.69*		0.83*
($\bar{2}$38)	(111)A	56 °	0.53	0.56	0.95
($\bar{1}$25)	(111)A	49 °	0.84	0.66	1.28
(111)A	(001)	55 °	0.50	0.57	0.88
($\bar{1}$13)B	(001)	24 °	0.87	0.91	0.95
(031)	(001)	72 °	0.42	0.31	1.33
(045)	(001)	38 °	0.71	0.79	0.90
(013)	(001)	19 °	0.90	0.94	0.96

*In coexistence with the ($\bar{2}$38) facet.

Table 1 summary of relative growth rates of the facets.

Substrate	Facet	Sidewall	Orientation dependence
(111)A	$(1\bar{1}4)$A	(001)	$\lambda_{Ga}(001) < \lambda_{Ga}(114)A \approx \lambda_{Ga}(111)A$
(001)		(111)A	
(111)A	$(11\bar{1})$B		$\lambda_{Ga}(001) < \lambda_{Ga}(\bar{1}\bar{1}\bar{1})B \leqq \lambda_{Ga}(111)A$
(001)	$(\bar{1}11)$B	Inverted mesa	
(001)	(011)		$\lambda_{Ga}(001) < \lambda_{Ga}(\bar{3}\bar{3}\bar{1})B < \lambda_{Ga}(111)A < \lambda_{Ga}(110)$
(111)A	(110)	$(33\bar{1})$B	
	$(\bar{1}01)$	Inverted mesa	$\lambda_{Ga}(111)A \approx \lambda_{Ga}(110)$
(111)A	(113)A		$\lambda_{Ga}(113)A < \lambda_{Ga}(111)A$
	$(\bar{1}\bar{1}3)$A		
(111)A	(159)		$\lambda_{Ga}(111)A \approx \lambda_{Ga}(159)$
(001)	$(\bar{1}13)$B		$\lambda_{Ga}(001) \approx \lambda_{Ga}(\bar{1}\bar{1}\bar{3})B$
(001)	(013)		$\lambda_{Ga}(001) < \lambda_{Ga}(013)$

Table 2 summary of orientation dependences of the Ga surface diffusion length.